Water Air Soil Pollut (2015) 226: 315
DOI 10.1007/s11270-015-2581-5

Sustainable Treatment of Antibiotic Wastewater Using Combined Process of Microelectrolysis and Struvite Crystallization

Jishi Zhang · Shujun Chen · Xikui Wang

Received: 11 June 2015 / Accepted: 11 August 2015 / Published online: 28 August 2015

Abstract The aim of this study was to investigate the synergistic effects of the process of iron-carbon microelectrolysis (ICME) followed by struvite (MAP) crystallization on treating antibiotic wastewater. Characteristics of ICME effluent depended mainly on the iron to carbon mass ratio (Fe/C). The optimum reaction conditions of Fe/C ratio of 2:1 and reaction time of 90 min were observed. The ICME effluent was further treated by MAP crystallization using $Na_2HPO_4 \cdot 12H_2O$ and $MgCl_2 \cdot 6H_2O$ as precipitation agents. The results showed that, the Mg^{2+}/NH_4^+-N/PO_4^{3-}-P molar ratio of 1:1:1 and pH 8.5, were suitable for the crystallization process, which could obtain high-quality MAP containing 5.18 % N,10.23 % Mg, and 13.83 % P. Optimal total removal rate of COD and NH_4^+-N removal rate achieved 84.6 and 89.9 %, respectively. The economic evaluation of NH_4^+-N recovery by the synergistic process was also conducted, indicating that the synergistic process had the potential to benefit COD emission reduction and nitrogen recovery.

Keywords Antibiotic wastewater · Iron-carbon microelectrolysis · Struvite crystallization · Sustainable mechanisms

Highlights
- Effects of Fe/C mass ratio on treatment efficiencies of antibiotic wastewater.
- 7-ADCD or 7-ACA was partly transformed into NH_4^+-N by microelectrolysis.
- NH_4^+-N concentrated was further recovered by struvite crystallization.
- MAP properties depended on Mg^{2+}/NH_4^+-N/PO_4^{3-}-P molar ratio and pH.
- N- and P-rich MAP could be used as a slow-release fertilizer.

J. Zhang (✉)
School of Environmental Science and Engineering,
Qilu University of Technology, Jinan 250353, China
e-mail: lyzhangjishi@163.com

S. Chen · X. Wang
School of Chemistry and Pharmaceutical Engineering,
Qilu University of Technology, Jinan 250353, China

1 Introduction

With the large demand for human and animal antibiotic drugs, antibiotics, in particular cephalosporins, have reached more than 60 species and accounted for more than 60 % of antibiotic production globally due to their effectiveness and low toxicity. Furthermore, antibiotics compounds and other drugs have been observed in the aquatic environment (Elmolla and Chaudhuri 2012; Jain et al. 2013). This may be resulted in the development of antibiotic resistant bacteria owing to the presence of antibiotics at low concentration in the environment (Walter and Vennes 1985). Antibiotic wastewater is of a special kind of wastewater with high concentrations of organic substances, antibiotic residues, and other pollutants (Yu et al. 2014). In addition, as shown in Fig. 1, a large number of cephalosporin intermediates, such as seven-amino-desacetoxy-cephalosporanic acid (7-ADCA) (formula: $C_8H_{10}N_2O_3S$, molecular weight= 214.24 g/mol) and seven-amino-cephalosporanic acid (7-ACA) (formula: $C_{10}H_{12}N_2O_5S$, molecular weight=

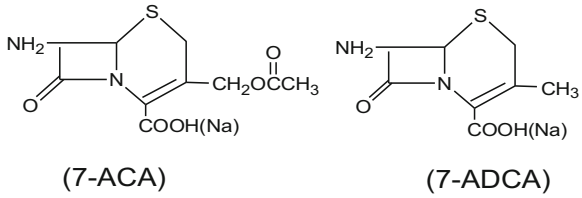

Fig. 1 Molecular structure of 7-ACA and 7-ADCA

272.28 g/mol), are necessary to synthesize antibiotics. Currently, 7-ADCA is generated approximately 1.0×10^5 t annually in China, which ranks the top in the world. Approximately 150–200 m^3 of antibiotic wastewater is produced from 1 t of antibiotic products (Yu et al. 2014). The technologies of antibiotic production include chemical synthesis, biological fermentation, and chemical-biological process. Antibiotic wastewater commonly contains many refractory chemicals such as toxic organic compounds, acids, and salts. Especially, high levels of ammonia nitrogen (NH_4^+-N) and organic nitrogen wastewater are always difficultly to be biodegraded. Although photocatalysis technologies can destroy molecular structure of 7-ACA (or 7-ADCA) and improve the biodegradability of this wastewater, some photocatalysts require high cost and complicated procedures. Moreover, among these pollutants, NH_4^+-N is also a major concern, which has a harmful effect on the local ecology such as depleting much of dissolved oxygen in water, causing eutrophication exacerbation (Lopata et al. 2006).

However, nitrogen (N) loss has become increasingly severe due to the excessive dosage and low efficiency of fertilizers containing N (Zheng et al. 2013), and therefore, they should be properly removed from wastewater before entering into aquatic systems (Ryu, et al. 2008). It could be inadequate to biologically treat antibiotic wastewater containing high concentration of NH_4^+-N and strong acidity since this wastewater has various toxic substances that inhibit active nitrification by nitrifying bacteria. Therefore, biological treatment processes have no effect on the degradation of antibiotic wastewater due to its significant toxicity to microorganisms in biological wastewater treatment; some pretreatment approaches are required to improve the biodegradability of this wastewater. Various physical and chemical processes or a combination of these approaches can be applied to treat this water with high NH_4^+-N content and high biotoxicity, which include air stripping, ion exchange, membrane separation, advanced oxidation, and chemical precipitation processes (Hao et al. 2008; Uludag-Demirer and Othman 2009).

On the one hand, for toxic and poor biodegradable substances in acid-antibiotic wastewater, some advanced oxidation processes are needed to reduce its acidity and removal toxics or change to biodegradable substances. The pretreatment approaches to convert the initially persistent organic compounds into more biodegradable intermediates could subsequently favor the biological treatment processes. Therefore, in order to avoid unnecessary expenditure of chemicals and energy, the level of mineralization should be suitable during the pretreatment stage, accordingly lowering the operating cost (Oller et al. 2011). Compared to conventional remediation techniques the iron-carbon microelectrolysis (ICME) has been regarded as a highly competitive water treatment technology treating the organic pollutants with high chemical stability and low biodegradability (Oller et al. 2011; Yang 2009; Ying et al. 2013). Previous studies have found that the ICME process treating pharmacy wastewater (Liu et al. 2015) and dye wastewater (Huang, et al. 2013) has energy-saving and cost-effective. As shown in Table 1 and described below, the mechanisms of removal organic pollutants are mainly reflected in numerous microscopic galvanic cells which are formed between the particles of iron and carbon when contacted with wastewaters (electrolyte solution) (Yang 2009; Wu, et al. 2011; Ruan, et al. 2010). Consequently, the efficiency of ICME depends mainly on the fundamental technological parameters, e.g., iron carbon mass ratio (Fe/C), pH, and aeration. Products released from the galvanic cell reaction including hydroxyl, atomic hydrogen, and Fe^{2+} have high activities to decompose contaminants (Yang 2009). The electrons are supplied from the galvanic corrosion of many microscale sacrificial anodes instead of external power supply (Wu, et al. 2011).

On the other hand, magnesium ammonium phosphate hexahydrate (MAP: $MgNH_4PO_4{\cdot}6H_2O$) can be applied for nitrogen removal or recovery from wastewater (Diwani et al. 2007). However, the key feature of this recovery technique is the combined removals of NH_4^+-N, phosphate (PO_4^{3-}-P), and magnesium (Mg^{2+}) from supersaturated solutions (Yetilmezsoy and Sapci-Zengin 2009). MAP could be always precipitated as a stable white orthorhombic crystal at the theoretical ratio (Mg^{2+}/NH_4^+-N/PO_4^{3-}-P=1:1:1) according to Eq. (1) (Nelson et al. 2003). Nevertheless, crystallization tests have shown that MAP precipitation reduces the pH of

Table 1 Half cell reactions of Fe-C microelectrolysis

Electrodes	Reactions	Oxidation-reduction potentials
Anode (Iron)	$Fe^{2+}(aq) + 2e \rightarrow Fe(s)$	$E^0\left(^{Fe^{2+}}/_{Fe}\right) = -0.44\ (V)$
	$Fe^{3+}(aq) + e \rightarrow Fe^{2+}(aq)$	$E^0\left(^{Fe^{3+}}/_{Fe^{2+}}\right) = 0.77\ (V)$
Cathode (Carbon) When aeration	Acidic $2H^+(aq) + 2e \rightarrow 2[H] \rightarrow H_2(g)$	$E^0\left(^{H^+}/_{H}\right) = 0.00\ (V)$
	Acidic $O_2(g) + 4H^+(aq) + 4e \rightarrow 2O + 4[H] \rightarrow 2H_2O(aq)$	$E^0(^{O_2}/_{H_2O}) = +1.23\ (V)$
	Acidic $O_2(g) + 2H^+(aq) + 2e \rightarrow H_2O_2(aq)$	$E^0(^{O_2}/_{H_2O_2}) = +0.68\ (V)$
	Neutral to alkaline $O_2(g) + 2H_2O(aq) + 4e \rightarrow 4OH^-(aq)$	$E^0(^{O_2}/_{OH^-}) = +0.40\ (V)$

the solution, and therefore, HPO_4^{2-}-P will take place in the reaction rather than PO_4^{3-}-P as Eq. (2) (Celen and Turker 2001).

$$Mg^{2+} + NH_4^+ + PO_4^{3-} + 6H_2O \rightarrow MgNH_4PO_4{\cdot}6H_2O \quad (1)$$

$$Mg^{2+} + NH_4^+ + HPO_4^{2-} + 6H_2O \rightarrow MgNH_4PO_4{\cdot}6H_2O + H^+ \quad (2)$$

Moreover, MAP solubility decreases with pH increasing, which indicates its precipitating potential increases. However, alkaline pH could not lead to formation of pure MAP; even no MAP existed at high pH (above 10.0) due to the existence of Ca^{2+} in solution (Wang et al. 2010). Therefore, both Mg^{2+}/NH_4^+-N/PO_4^{3-}-P ratio and pH play important roles in MAP crystallization process.

In this study, an innovative approach was used to synergistically treat antibiotic wastewater and recovery NH_4^+-N using the combined process of ICME and MAP crystallization (Fig. 2). The specific objectives were as follows:

1. Investigate the effects of ICME on the removal efficiency of COD, and the enrichment of NH_4^+-N that can be used as nitrogen source for MAP formation.
2. Optimize key parameters such as Mg^{2+}/NH_4^+-N/PO_4^{3-}-P mass ratio, hydraulic retention time (HRT), and pH in order to form MAP and recycle NH_4^+-N in the effluents of ICME from antibiotic wastewater.
3. Assess the benefits of NH_4^+-N emission reduction and NH_4^+-N recovery from the sustainable treatment of antibiotic wastewater.

Interestingly, when the ICME unit is to be followed by MAP crystallization process, the synergistic effects on nitrogen recovery and COD reduction have more practical advantages than other treatment technologies. Besides, to the best of our knowledge, the synergistic process of ICME followed by MAP crystallization is reported here for the first time.

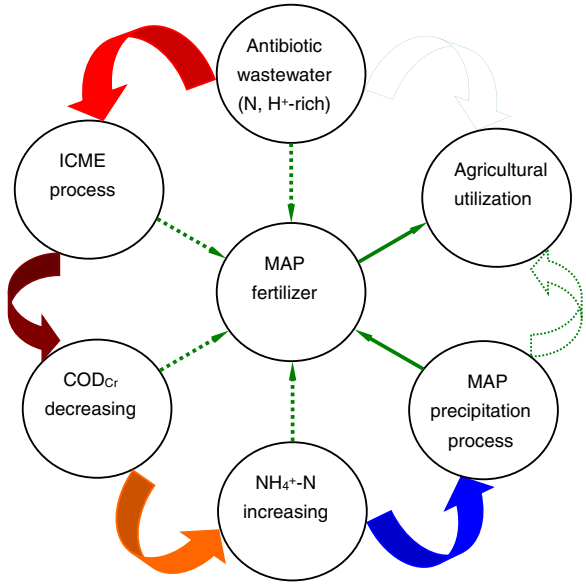

Fig. 2 The combined process of ICME and MAP crystallization treating antibiotic wastewater

2 Materials and Methods

2.1 Characteristics of Antibiotic Wastewater

Antibiotic wastewater samples were obtained from the Shandong New Times Pharmaceutical Co., Ltd. (China). The characteristics of antibiotic wastewater are given in Table 2. Significantly, high concentrations of NH_4^+-N, COD, and low pH values were observed.

2.2 Experimental Procedure

The iron scrap samples were collected from the Metalworking Practice Factory in Qilu University of Technology, China, which were used in ICME process. The iron scrap samples were firstly degreased in a 10 % NaOH solution for 30 min, then soaked in a diluted (5 %) hydrochloride acid solution for 60 min to remove rust, and finally cleaned by deionized water and vacuum-dried before used. Fe particle sizes are between 2 and 4 mm, while the particle of activated carbon obtained from an activated carbon company in Shandong has a size range of 3.0–5.0 mm.

For ICME, the reactor was aerated through a diffuser on the bottom of reactor with working volume 1000 ml, and oxygen was provided by compressed air keeping at 2.0 mg/L, approximately. The total weight of Fe-C bed of 150 g with different ratios of iron to carbon (Fe/C, 1–4), and wastewater were added into a reactor, keeping HRT for 90 min.

The ICME effluents were further treated through the struvite crystallization process after pH was adjusted to 8.0. Magnesium chloride ($MgCl_2 \cdot 6H_2O$) was used with a concentration of 30 g Mg^{2+}/L as the magnesium source. For the phosphate source, a sodium phosphate ($Na_2HPO_4 \cdot 12H_2O$) stock solution containing 30 g PO_4^{3+}-P/L was also prepared. MAP reaction lasted for about 20 min until an equilibrium state reached as indicated by a stable pH. NaOH solution (10 M) was used for pH adjustment. All experiments described in this study were performed in triplicate, and all results were the average of replicate analysis.

2.3 Analytical Methods

Chemical oxygen demand (COD), total Kjeldahl nitrogen (TKN), ammonia nitrogen (NH_4^+-N), and pH were all determined according to standard methods (APHA, 1999). Metal ion concentrations were measured by inductively coupled plasma optical emission spectroscopy (ICP-OES) analysis, using an Optima 3000 instrumentation (Perkin- Elmer). The surface structure of struvite was conducted by the field-emission scanning electron microscope (KYKY-3800B, China), and micrographs are shown in following sections. The analyses of MAP composition were determined by energy-dispersive spectroscopy (EDS, Oxford Model 5526), with an accelerating voltage of 10.0 kV. Fourier transform infrared (FT-IR) spectrometry of MAP samples were collected by FT-IR spectroscopy (IRPrestige-21, Schimadzu, Japan), which covered the infrared region 4000–400 cm^{-1}.

3 Results and Discussion

3.1 Effects of Microelectrolysis on COD and NH_4^+-N Removals

Although the ICME reactor was composed of numerous carbon and iron particles, it was simplified to a single couple of iron scrap and graphite in order to investigate the details of its electrochemical behavior (Ying et al. 2013). Fe and C form a galvanic couple resulting in oxidation of Fe and reduction of oxygen to water. Electrochemical reaction between Fe and C in the antibiotic wastewater is an electrochemical corrosion process. During the ICME process, aeration, pH and Fe/C have strong influences on effluent pH, COD removal, 7-ADCA/7-ACA transformation, and NH_4^+-N concentration. It was obvious that the organic pollutants mainly including 7-ACA and 7-ADCA could be oxidized or reduced by radicals and oxidants such as free hydrogen [H] or O· produced from electrode action (Lai, et al. 2013), as described in Table 1. The NH_4^+-N in effluent

Table 2 Characteristics of raw antibiotic wastewater

COD (mg L^{-1})	NH_4^+-N (mg L^{-1})	TKN (mg L^{-1})	pH	Chrominance	Salinity (g L^{-1})	Density (kg m^{-3})
7900±100	3460±50	6340±50	2.4±0.2	50±10	13.0±0.5	1010±20

of ICME process were detected to increase, while COD were measured to decrease in whole running process, which indicated that the degradation products could be the smaller molecule organics and inorganic nitrogen (e.g., NH_4^+-N). Moreover, the antibiotics were also removed through adsorption and reduction of granular carbon particles. This could be explained by the fact that, in the ICME system there were enough H^+ ions on the surface of the carbon to accept the electrons to generate [H], and that the 7-ACA or 7-ADCA on the surface of carbon could be reduced by the generated [H] and turned into intermediate products and end products. These products mainly included smaller molecule organics and NH_4^+-N. Furthermore, the 7-ACA (or 7-ADCA) destruction in the anode cell could be due to the reduction by ferrous iron and leakage of current (Ying et al. 2013). Additionally, aerial oxidation of antibiotics with Fe and C providing a heterogenous interface to catalyze the reaction could occur, which resulted in improving organic contaminant decomposition. In electro-Fenton heterogeneous system, a significant synergetic effect between anodic oxidation and single Fe-C microelectrolysis was attributed to the effective electro-Fenton oxidation at favorable acidic pH condition that triggered by anodic oxidation (Zhang et al. 2015). Therefore, the removal and destruction of characteristic organic pollutants such as 7-ACA and 7-ADCA were mainly reflected in the COD and NH_4^+-N variations in effluent of ICME process.

Since the corrosion reaction of iron was affected greatly by H^+ concentration, the influent pH is an important parameter that affects the kinetics in the pretreatment process by the ICME (Lai et al. 2012; Liu et al. 2007). It was also observed that influent pH affects the activity of oxidant and substrate, the speciation of iron (Table 1). According to Nernst equation, the reaction rate of $Fe \rightarrow Fe^{2+}$ increases with an increase of the H^+ concentration; thus, the destruction of 7-ACA or 7-ADCA could be affected seriously by the influent pH of ICME. However, the pH changes of microelectrolysis reactions at different Fe/C ratios showed a similar tendency that pH values increased sharply from 2.4 to about 5.0 in the first 30 min, finally being stable at around 6.6 after 120 min (Fig. 3).

This is why the microelectrolysis process consumes acid. The stronger acidic aqueous solution is, the larger the battery potential differences between anode (iron) and cathode (carbon) will be. Furthermore, the aeration enhances the oxidation of Fe^{2+} to Fe^{3+}, which accompanies the production of basicity as Eq. (3).

$$4Fe^{2+} + O_2 + 2H_2O \rightarrow 4Fe^{3+} + 4OH^- \quad (3)$$

Nevertheless, the increase of pH improves the production of $Fe(OH)_2$ and $Fe(OH)_3$ at the same time, which could restrain the increase of pH. The same thing also occurs when HRT is long. After the reactions balance, the pH of the ICME effluent is near neutral (Yang 2009).

As shown in Fig. 4, an increase in Fe/C mass ratio generally improved COD removal efficiencies that were in the range of 8.9–70.0 %. The highest COD removal efficiency and NH_4^+-N concentration reached to 70.0 % and 4890 mg/L at Fe/C mass ratio of 2, respectively. The mass transfer rate of oxygen in the Fe/C layer could decrease when Fe/C ratios exceeded 2:1. The mass transfer in bubble-aerated ICME process depended on the amount, size, breakup, and coalescence of gas bubbles. Higher Fe/C layer could cause an increase in oxygen transfer resistance at a given aeration rate (2.0 mg/L). Therefore, this phenomenon could hinder the effective contact between Fe and C and decrease the reaction rate of cathode (carbon), resulting in a decrease in the COD removal from antibiotic wastewater. The results indicate that methods of suitable aeration and Fe/C ratio enhance COD removal and refractory compound degradation in ICME unit. Similarly, it was found that ICME reactor could not remove organic nitrogen, but it could transform the organic nitriles into NH_4^+-N, amine and acylamide, and the NH_4^+-N transformation efficiency reached 50 % when the influent pH and Fe/C ratio were 4 and 1:1 (*v*/*v*), respectively (Liu et al. 2007).

The COD removal in the ICME unit was likely due to galvanic cells reaction, when a mixture of iron chips and activated carbon particles was in contact with wastewaters; numerous microscopic galvanic cells were formed between the particles of Fe and C. In the ICME unit, the iron particles, as an anodic metal, provided electrons for the destruction of characteristic organic pollutants; meanwhile, carbon particles were used as cathodes to form a large quantity of macroscopic galvanic cells by the contact with iron particles, and strongly increase the current efficiency of the ICME unit (Liu et al. 2007). Furthermore, these substances released from galvanic cell reaction had high activities that can easily remove, transform, and degrade organic pollutants. According to Table 1, when aeration Fe was first oxidized into Fe^{2+}

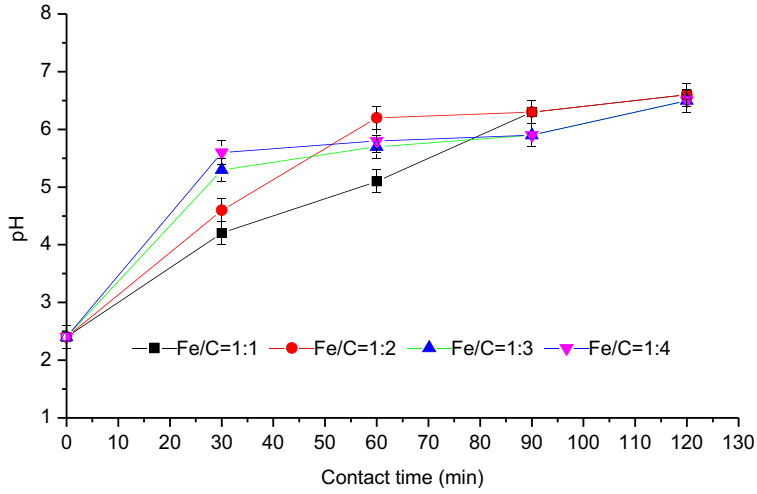

Fig. 3 Effects of Fe/C ratio on pH

and then oxidized to Fe^{3+} along with hydroxyl radical formation (Cheng et al. 2007; Johnston and Singer 2007). Organic pollutants are consequently broken into small molecule substances due to the strong oxidization property of hydroxyl radical (Yang 2009). Furthermore, Fe^{3+} mainly precipitates as $Fe(OH)_3$ when the pH value of solution is higher than 4, the flocculation precipitation processes from $Fe(OH)_3$ will lead to further disposal of organic contaminants (Yang 2009).

It was clear that the NH_4^+-N content was concentrated through the ICME unit, which ranged from 3460 to 4890 mg/L (Fig. 4). This indicated that the macroscopic galvanic cells predominated in decomposition and transformation of 7-ADCA or 7-ACA from cephalosporin antibiotic wastewater. The contaminants containing big molecule organic nitrogens (e.g., 7-ADCA or 7-ACA) could be decomposed into the inorganic nitrogens (e.g., NH_4^+-N) and small molecule organic nitrogens, not only by redox reaction and flocculation in the result of $Fe(OH)_2$ and $Fe(OH)_3$ but also by electrophoresis under electric fields created by electron flow. Interestingly, the increase of final NH_4^+-N concentration further favored MAP crystallization and NH_4^+-N recovery.

Nevertheless, ICME process was also inhibited by high pH resulting from the increase of Fe/C ratio. Particularly, the COD removal of ICME obviously decreased when the Fe/C ratios were higher than 2. Therefore, the ICME system with Fe/C ratio of 2 should be more economical, effective, and feasible for application of ammonium removal through MAP crystallization than others. Besides, when the ratios were above 2, the amount of floc could increase, and floc particles could become smaller, consequently restraining the flocculation process, thus reducing COD removal and TKN transform (Zhang et al. 2015; Lai et al. 2013).

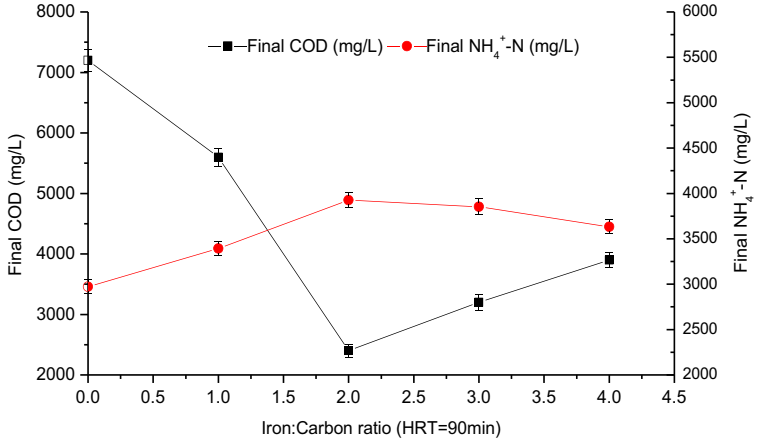

Fig. 4 Effects of Fe/C ratios on final concentrations of COD and NH_4^+-N

Regarding above results, the main conclusions were obtained that the ICME reactor could transform the toxic organic pollutants (7-ACA and 7-ADCA) in antibiotic wastewater into less toxic by-products, and the degradation of toxic organic pollutants was attributed to the macroscopic galvanic cells in the ICME reactor. Furthermore, increases in the NH_4^+-N concentration and COD removal efficiency of ICME effluent, further contributed to MAP precipitation, which subsequently favored the bio-treatment process of this wastewater.

3.2 Effects of MAP Precipitation on COD and NH_4^+-N Removals

The success of MAP precipitation depends on two primary factors: Mg^{2+}/NH_4^+-N/PO_4^{3-}-P ratio and solution pH (Münch and Barr 2001). H^+ concentration does not directly enter the ion activity product equation, but MAP precipitation is highly pH dependent because the activities of both NH_4^+ and PO_4^{3-} are pH dependent (Nelson et al. 2003). pH plays an important role during MAP precipitation process. Although MAP can be precipitates at a wide range of pH (7.0–11.5), the suitable pH ranges from 7.5 to 9.0 (Hao et al. 2008). MAP is soluble in diluted acid, and insoluble in alkaline solution. Therefore, the crystallization reaction should be controlled under alkaline conditions. In MAP precipitation tests at room temperature, it was observed that the initial pH 8.0 of effluent from microelectrolysis system with the Fe/C ratio of 2, dropped immediately to 6.6, as soon as the chemicals were added at the Mg^{2+}/NH_4^+-N/PO_4^{3-}-P ratio of 1:1:1. It may be practical to control the Mg^{2+}/NH_4^+-N/PO_4^{3-}-P molar ratio of 1:1:1 when the NH_4^+-N is required to be precipitated from high level of NH_4^+-N in wastewaters from an engineering point of view (Yetilmezsoy and Sapci-Zengin 2009; Li et al. 1999). The possible reason is that the formation of MAP requires the presence of Mg^{2+}, NH_4^+-N, and PO_4^{3-}-P with a theoretical molar ratio of 1:1:1, and that high concentration of NH_4^+-N will better combine with Mg^{2+} and PO_4^{3-}-P to formed MAP (Yetilmezsoy and Sapci-Zengin 2009; Bi et al. 2014; Huang and Liu 2014). In order to minimize the NH_4^+-N residual concentration in the microelectrolysis pretreated effluent, the pH was raised gradually by adding 5 and 10 M NaOH solution to adjust final pH 10, respectively. As the pH was increased above its initial value, the removal percentage of the residual NH_4^+-N significantly increased and reached its maximum value at pH 8.5; When the pH was further rising from 9 to 10, the residual NH_4^+-N concentrations slightly decreased (Fig. 5). In addition, some impurities such as $Mg(OH)_2$ and $Mg_3(PO_4)_2$ probably emerged in the precipitations at pH of higher than 9. A similar result also showed that 73.3 % NH_4^+-N was removed and recovered as MAP at pH 8.5 and at stoichiometric ratio ($Mg^{2+}/NH_4^+/PO_4^{3-}$= 1:1:1), and that removal efficiency of NH_4^+-N did not improve when molar ratio became higher than stoichiometry (Huang and Liu 2014).

In these tests, the effluent quality in terms of the residual COD was also determined, indicating that MAP precipitation help to remove 92.8 % of NH_4^+-N from the microelectrolysis pretreated effluent, and to achieve maximum removal efficiency of 49.3 % for COD. These phenomena were similar to the previous study that the best NH_4^+-N reduction was observed 89 % at pH 9.2, with corresponding COD removal of 50 % for anaerobically treated landfill leachate effluent used in a MAP precipitation process (Ozturk et al. 2003). The optimal total COD removal rate and NH_4^+-N reduction rate achieved 84.6 and 89.9 %, respectively.

It was reported that as HRT was increased from 1 to 180 min, crystal size was found to increase from 0.1 to 3 mm while the removal rates of NH_4^+-N and PO_4^{3-}-P increased only by 4 % (Stratful et al. 2001). In order to determine the morphology, the MAP precipitate generated from the microelectrolysis pretreated effluent by adding $Na_2HPO_4{\cdot}12H_2O$ and $MgCl_2{\cdot}6H_2O$ was examined by a scanning electron microscope (SEM), and the SEM micrograph is shown in Fig. 6. Results indicated that the struvite was orthorhombic crystal, and level sex was better, crystal wedge-shaped or thick plates, with good crystal morphology, structure, and high purity.

Similar results were found in previous studies that MAP crystals had a similar shape to its seed crystals, indicating that there was no phase transformation during growth (Mehta and Batstone 2013). The crystal size of MAP precipitate was in range of 10–50 μm, mainly depending on the competition between nucleation and crystal rates (Mehta and Batstone 2013). The final product crystal size distributions were uniform, indicating a good product quality. However, the morphology of developed crystal normally depended upon the supersaturation of the solution together with the concentration of impurities (Li and Zhao 2003). Besides, regulation of pH remained the most important role in preventing side reactions such as magnesium hydroxide (pK_s=11.16) or magnesium hydrogen phosphate (pK_s=5.8)

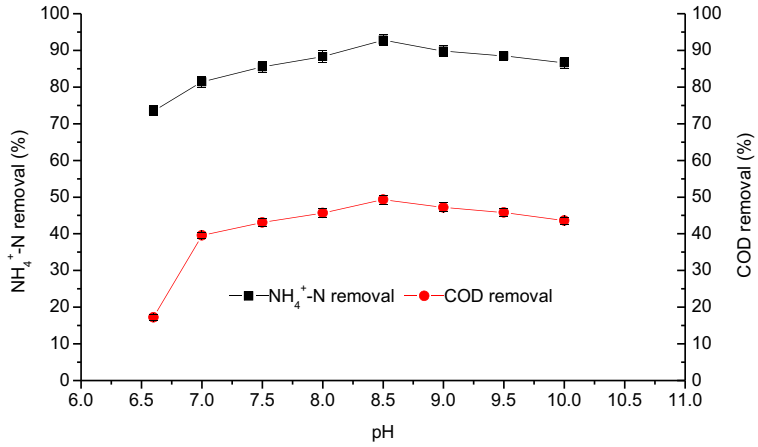

Fig. 5 Effect of pH on NH_4^+-N, COD removals from the ICME pretreated effluents for different chemical combinations (initial NH_4^+-N=4890 mg/L, initial COD=2400 mg/L, initial pH=8.5, Mg^{2+}/NH_4^+-N/PO_4^{3-}-P=1:1:1)

precipitation (Li and Zhao 2003). Furthermore, MAP was sparingly soluble in neutral and alkaline conditions, but readily soluble in acid condition.

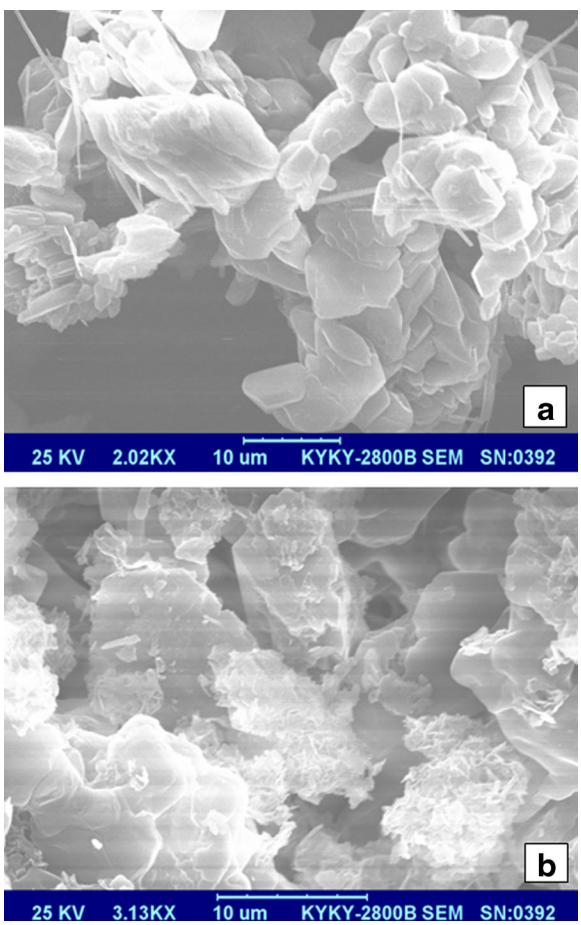

Fig. 6 SEM photographs of MAP precipitates at different magnifications. **a** 2.02 k×, and **b** 3.13 k×, generated at pH 8.5 with Mg^{2+}/NH_4^+-N/PO_4^{3-}-P=1:1:1

FT-IR spectroscopy is an important and common technique to determine the chemical structure, chain orientation, and composition of different compounds (e.g., organic, inorganic, and polymeric in nature). FT-IR spectra and spectroscopic assignment of the MAP samples showed changes of the functional groups on the surfaces of the MAP derived from Mg^{2+}/NH_4^+-N/PO_4^{3-}-P ratio of 1:1:1 at pH 8.5. The FT-IR characteristics of MAP are described in Table 3, with the comparison of previous literature data. Peaks 1–5 (3800–2200 cm^{-1}) contributed to O-H and N-H stretching. The visible peaks at 1684, 1620, and 1436 cm^{-1} indicated the presence of NH_4^+, while the visible peaks at 1005, 920, 772, and 571 cm^{-1} were attributed to the presence of PO_4^{3-}-P. These phenomena agreed with the FT-IR spectra of MAP crystals reported in previous studies (Stefov et al. 2005; Su et al. 2014).

The chemical properties of the MAP precipitate were also determined by an energy-dispersive spectroscopy. The results indicated that it had a composition of 5.18 % N, 10.23 % Mg, and 13.83 % P when the Mg^{2+}/NH_4^+-N/PO_4^{3-}-P molar ratio of 1:1:1 was used, which was close to the theoretical composition 5.7 % N, 9.9 % Mg, and 12.6 % P of standard MAP (Münch and Barr 2001). This indicated that the effects of Ca-P precipitation and ion exchange reactions of MAP formation were negligible (Yin and Kong 2014). Therefore, the ICME effluent reacted with Mg^{2+} and PO_4^{3-}-P and formed MAP precipitate that could be used as slow-release fertilizers for horticulture and agriculture (Yetilmezsoy and Sapci-Zengin 2009). There is an active interest to produce struvite on commercial scale in Japan. However, local availability and price of chemicals, and the price of use and selling of MAP will determine whether this process

Table 3 Comparison of the observed absorption peaks of MAP

Peak number	Observed values (cm^{-1}) This study	Reported values (cm^{-1})		Bonds/vibrations
		Stefov et al. (2005)	Su et al. (2014)	
1	3582	3800–2200	3587	O-H, N-H stretching
3	3478	3800–2200	3480	O-H, N-H stretching
3	3265	3800–2200	3256	O-H, N-H stretching
4	2952	3800–2200	2943	O-H, N-H stretching
5	2365	3800–2200	2353	O-H, N-H stretching
6	1620	1702	1615	NH_4^+ ν4 bending
7	1684	1685	1683	NH_4^+ ν4 bending
8	1436	1442	1439	NH_4^+ ν2 bending
9	1005	1006	1004	PO_4^{3-} ν3 bending
10	920	940	896	PO_4^{3-} ν4 bending
11	772	780–570	761	PO_4^{3-} ν2 bending
12	571	780–570	570	PO_4^{3-} ν2 bending

can potentially compete with alternative nitrogen removal or recovery technologies currently available in the market (Türker and Çelen 2007).

3.3 Economic Evaluation

Although antibiotic wastewater shows acidic, the wastewater can flow into ICME unit directly without adjustment on pH because ICME can adapt wastewater in wide range of pH. The effluent pH of ICME increased from 2.4 to about 6.6 for 120 min (Fig. 3), while NH_4^+-N concentration increased from 3460 to 4890 mg/L (Fig. 4). Results suggest that ICME is an effective and economic pretreatment method for acidic-antibiotic wastewater, which provide a comfortable environment for MAP crystallization. Antibiotic wastewater is rich in nitrogen that can be recovered to form MAP, while the utilization of MAP as an effective fertilizer would favor the reduction of the application of rock phosphate in the agricultural sector. Besides, MAP precipitation in wastewater and for reuse and NH_4^+-N emission reduction can reduce cost and may be a safe practice for sustainable environmental nutrient management (Miyittah et al. 2012), and sustainable treatment of the wastewater enriching with N and P. Rate of N release also depends on the MAP particle size. The smaller particle sizes released more N than the bigger particles. It is possible to remove 40 % N (Rahman et al. 2014) and 93 % P (Rahman et al. 2011) through MAP crystallization from wastewaters. Furthermore, its selling price can counteract the costs of sodium phosphate and sodium hydrate consumed during the processes of ICME technology and MAP crystallization. Besides, economic evaluation of NH_4^+-N recovery by the ICME combined with MAP precipitation was conducted, which took only chemicals cost (i.e., $MgCl_2{\cdot}6H_2O$, $Na_2HPO_4{\cdot}12H_2O$, and NaOH) into account. The cost of ICME treating 1 t this wastewater is about \$0.2–0.5 that is omitted, while approximately 5 kg NH_4^+-N is accordingly obtained. Theoretically, the recovery of 1.0 kg NH_4^+-N needs to consume 1.71 kg Mg, 2.21 kg P, and a small amount of NaOH, with according to MAP production of 7.59 kg. The current market prices of $MgCl_2{\cdot}6H_2O$ and $Na_2HPO_4{\cdot}12H_2O$ are about 80 and 810 dollars per ton, respectively. The recovery of NH_4^+-N costs approximately \$870 t^{-1}, while the price of MAP per ton reached \$200–350. Therefore, MAP precipitation is simultaneously beneficial for the humankind for providing high-quality and slow-releasing fertilizers, and decreasing the risk of water and soil pollution through recovering of nitrogen element from wastewater.

Furthermore, the combined process of ICME and MAP crystallization is economically viable for nitrogen removal and recovery from antibiotic wastewater, as compared with other traditional treatment technologies such as evaporation method. The cost of triple effect evaporation treating 1 t this wastewater is \$15–20 (40 % total solid) without considering the cost of wastewater pH regulation. The evaporated residue has been classified as toxic industrial waste, which needs to be treated

before discharge. The posttreatment cost of the evaporated residue is about $320 (0.4 t). As calculated from Table 2, recovering 1 t NH_4^+-N requires approximately 200 t this wastewater to evaporate, which cost approximately 68,000 dolls. Thus, the cost of evaporation of 1 t NH_4^+-N is about 78 times as much as that of the process of ICME followed by MAP precipitation, indicating that the synergistic process has the potential to benefit COD emission reduction and nitrogen recovery.

4 Conclusions

The characteristics of ICME effluent depended mainly on the iron to carbon ratio (Fe/C). The optimum reaction conditions were observed at iron/carbon mass ratio of 2:1 and aeration reaction time of 90 min. The ICME effluent was further treated by MAP precipitation using $Na_2HPO_4 \cdot 12H_2O$ and $MgCl_2 \cdot 6H_2O$ as precipitation agents. Results indicated that, the Mg^{2+}/NH_4^+-N/PO_4^{3-}-P molar ratio of 1:1:1 and pH 8.5 were better for MAP crystallization, obtaining MAP with high purity and good crystal morphology with 5.18 % N, 10.23 % Mg, and 13.83 % P. Total removal rates of COD and NH_4^+-N reduction rates achieved 84.6 and 89.9 %, respectively. The understanding and optimization of nitrogen recovery process by the ICME coupled with MAP crystallization will increase the development of sustainable processes.

Acknowledgments The authors would like to thank the anonymous reviewers for their insightful comments on the manuscript. Besides, this research was supported by the Shandong Province Science and Technology Development Program, China (grant no. 2013GSF11718), and Jinan Science and Technology Development Program, China (grant no. 201201136).

References

APHA. (1999). Standard methods for the examination of water and wastewater, 20th edn. Washington, DC: American public health association (APHA).

Bi, W., Li, Y., & Hu, Y. (2014). Recovery of phosphorus and nitrogen from alkaline hydrolysis supernatant of excess sludge by magnesium ammonium phosphate. *Bioresource Technology, 166*, 1–8.

Celen, I., & Turker, M. (2001). Recovery of ammonia as struvite from anaerobic digester effluents. *Environmental Technology, 22*(11), 1263–1272.

Cheng, H., Xu, W., Liu, J., Wang, H., He, Y., & Chen, G. (2007). Pretreatment of wastewater from triazine manufacturing by coagulation electrolysis, and internal microelectrolysis. *Journal of Hazardous Materials, 146*(1–2), 385–392.

Diwani, G. E., Rafie, S. E., El Ibiari, N. N., & El-Aila, H. I. (2007). Recovery of ammonia nitrogen from industrial wastewater treatment as struvite slow releasing fertilizer. *Desalination, 214*(1–3), 200–214.

Elmolla, E. S., & Chaudhuri, M. (2012). The feasibility of using combined Fenton-SBR for antibiotic wastewater treatment. *Desalination, 285*, 14–21.

Hao, X. D., Wang, C. C., Lan, L., & Von Loosdrecht, M. C. M. (2008). Struvite formation, analytical methods and effects of pH and Ca^{2+}. *Water Science and Technology, 58*(8), 1687–1692.

Huang, A. H., & Liu, J. C. (2014). Removal of ammonium as struvite from wet scrubber wastewater. *Water, Air, & Soil Pollution, 225*, 2062–2068.

Huang, L., Sun, G., Yang, T., Zhang, B., He, Y., & Wang, X. (2013). A preliminary study of anaerobic treatment coupled with micro-electrolysis for anthraquinone dye wastewater. *Desalination, 309*, 91–96.

Jain, S., Kumar, P., Vyas, R. K., Pandit, P., & Dalai, A. K. (2013). Occurrence and removal of antiviral drugs in environment: a review. *Water, Air, & Soil Pollution, 224*, 1410–1416.

Johnston, R. B., & Singer, P. C. (2007). Redox reactions in the Fe-As-O_2 system. *Chemosphere, 69*(4), 517–525.

Lai, B., Zhoua, Y., Qin, H., Wu, C., Pang, C., Lian, Y., & Xu, J. (2012). Pretreatment of wastewater from acrylonitrile-butadiene-styrene (ABS) resin manufacturing by microelectrolysis. *Chemical Engineering Journal, 179*, 1–7.

Lai, B., Zhou, Y., Yang, P., Yang, J., & Wang, J. (2013). Degradation of 3,30-iminobis- propanenitrile in aqueous solution by Fe^0/GAC micro-electrolysis system. *Chemosphere, 90*, 1470–1477.

Li, X. Z., & Zhao, Q. L. (2003). Recovery of ammonium-nitrogen from landfill leachate as a multi-nutrient fertilizer. *Ecological Engineering, 20*(2), 171–181.

Li, X. Z., Zhao, Q. L., & Hao, X. D. (1999). Ammonium removal from landfill leachate by chemical precipitation. *Waste Management, 19*(6), 409–415.

Liu, H. N., Li, G. T., Qu, J. H., & Liu, H. J. (2007). Degradation of azo dye Acid Orange 7 in water by Fe^0/granular activated carbon system in the presence of ultrasound. *Journal of Hazardous Materials, 144*(1–2), 180–186.

Liu, P., Zhang, H., Feng, Y., Shen, C., & Yang, F. (2015). Integrating electrochemical oxidation into forward osmosis process for removal of trace antibiotics in wastewater. *Journal of Hazardous Materials, 296*, 248–255.

Lopata, K. R., Auerswald, L. P., & Cook, P. (2006). Ammonia toxicity and its effect on the growth of the South Africa abalone *Haliotis midae* Linnaeus. *Aquaculture, 261*(2), 678–687.

Mehta, C. M., & Batstone, D. J. (2013). Nucleation and growth kinetics of struvite crystallization. *Water Research, 47*(8), 2890–2900.

Miyittah, M. K., Gadekar, S., Pullammanappallil, P., Stanley, C. D., Bonzongo, J. C., & Rechcigl, J. E. (2012). Application of polymath chemical equilibrium simulation model for struvite precipitation in soils. *Water, Air, & Soil Pollution, 223*, 995–2001.

Münch, E. V., & Barr, K. (2001). Controlled struvite crystallization for removing phosphorus from anaerobic digester side-streams. *Water Research, 35*(1), 151–159.

Nelson, N. O., Mikkelsen, R. L., & Hesterberg, D. L. (2003). Struvite precipitation in anaerobic swine lagoon liquid: effect of pH and Mg:P ratio and determination of rate constant. *Bioresource Technology, 89*(3), 229–236.

Oller, I., Malato, S., & Sánchez-Pérez, J. A. (2011). Combination of advanced oxidation processes and biological treatments for wastewater decontamination-a review. *Science of the Total Environment, 409*(20), 4141–4166.

Ozturk, I., Altinbas, M., Koyuncu, I., Arikan, O., & Gomec-Yangin, C. (2003). Advanced physico-chemical treatment experiences on young municipal landfill leachates. *Waste Management, 23*(5), 441–446.

Rahman, M. M., Liu, Y. H., Kwag, J. H., & Ra, C. S. (2011). Recovery of struvite from animal wastewater and its nutrient leaching loss in soil. *Journal of Hazardous Materials, 186*(2–3), 2026–2030.

Rahman, M. M., Salleh, M. A. M., Rashid, U., Ahsan, A., Hossain, M. M., & Ra, C. S. (2014). Production of slow release crystal fertilizer from wastewaters through struvite crystallization - A review. *Arabian Journal of Chemistry, 7*(1), 139–155.

Ruan, X. C., Liu, M. Y., Zeng, Q. F., & Ding, Y. H. (2010). Degradation and decolorization of reactive red X-3B aqueous solution by ozone integrated with internal micro-electrolysis. *Separation and Purification Technology, 74*(2), 195–201.

Ryu, H. D., Kim, D., & Lee, S. I. (2008). Application of struvite precipitation in treating ammonium nitrogen from semiconductor wastewater. *Journal of Hazardous Materials, 156*(1–3), 163–169.

Stefov, V., Šoptrajanov, B., Kuzmanovski, I., Lutz, H. D., & Engelen, B. (2005). Infrared and Raman spectra of magnesium ammonium phosphate hexahydrate (struvite) and its isomorphous analogues. III. Spectra of protiated and partially deuterated magnesium ammonium phosphate hexahydrate. *Journal of Molecular Structure, 752*(1–3), 60–67.

Stratful, I., Scrimshaw, M. D., & Lester, J. N. (2001). Conditions influencing the precipitation of magnesium ammonium phosphate. *Water Research, 35*(17), 4191–4199.

Su, C. C., Abarca, R. R. M., de Luna, M. D. G., & Lu, M. C. (2014). Phosphate recovery from fluidized-bed wastewater by struvite crystallization technology. *Journal of the Taiwan Institute of Chemical Engineers, 45*(5), 2395–2402.

Türker, M., & Çelen, I. (2007). Removal of ammonia as struvite from anaerobic digester effluents and recycling of magnesium and phosphate. *Bioresource Technology, 98*(8), 1529–1534.

Uludag-Demirer, S., & Othman, M. (2009). Removal of ammonium and phosphate from the supernatant of anaerobically digested waste activated sludge by chemical precipitation. *Bioresource Technology, 100*(13), 3236–3244.

Walter, M. V., & Vennes, J. W. (1985). Occurrence of multiple-antibiotic resistant enteric bacteria in domestic sewage and oxidative lagoons. *Applied and Environmental Microbiology, 50*(4), 930–933.

Wang, C. C., Hao, X. D., Guo, G. S., & van Loosdrecht, M. C. M. (2010). Formation of pure struvite at neutral pH by electrochemical deposition. *Chemical Engineering Journal, 159*, 280–283.

Wu, S., Qi, Y., Gao, Y., Xu, Y., Gao, F., Yu, H., Lu, Y., Yue, Q., & Li, J. (2011). Preparation of ceramic-corrosion-cell fillers and application for cyclohexanone industry wastewater treatment in electrobath reactor. *Journal of Hazardous Materials, 196*, 139–144.

Yang, X. (2009). Interior microelectrolysis oxidation of polyester wastewater and its treatment technology. *Journal of Hazardous Materials, 169*, 480–485.

Yetilmezsoy, K., & Sapci-Zengin, Z. (2009). Recovery of ammonium nitrogen from the effluent of UASB treating poultry manure wastewater by MAP precipitation as a slow release fertilizer. *Journal of Hazardous Materials, 166*, 260–269.

Yin, H., & Kong, M. (2014). Simultaneous removal of ammonium and phosphate from eutrophic waters using natural calcium-rich attapulgite-based versatile adsorbent. *Desalination, 351*, 128–137.

Ying, D., Peng, J., Li, K., Wang, Y., Pan, S., & Jia, J. (2013). Dual-cell reduction and group effect in an internal microelectrolysis reactor. *Electrochimica Acta, 89*, 861–867.

Yu, X., Zuo, J., Li, R., Gan, L., Li, Z., & Zhang, F. (2014). A combined evaluation of the characteristics and acute toxicity of antibiotic wastewater. *Ecotoxicology and Environmental Safety, 106*, 40–45.

Zhang, C., Zhou, M., Yu, X., Ma, L., & Yu, F. (2015). Modified iron-carbon as heterogeneous electro-Fenton catalyst for organic pollutant degradation in near neutral pH condition: Characterization, degradation activity and stability. *Electrochimica Acta, 160*, 254–262.

Zheng, H., Wang, Z., Deng, X., Herbert, S., & Xing, B. (2013). Impacts of adding biochar on nitrogen retention and bioavailability in agricultural soil. *Geoderma, 206*, 32–39.